



## Anti-icing efficiency on bio-inspired slippery elastomer surface

Nguyen Thanh Binh<sup>a,1</sup>, Vu Thi Hong Hanh<sup>a,1</sup>, Ngo Tuan Ngoc<sup>a</sup>, Nguyen Ba Duc<sup>b,\*</sup>

<sup>a</sup> Thai Nguyen University of Education, Thai Nguyen, Viet Nam

<sup>b</sup> Tan Trao University, Tuyen Quang, Viet Nam

### HIGHLIGHTS

- Have reinforced the ice repellency performance in several scenarios.
- Nanostructure exhibited a good affinity with low surface tension lubricant while maintaining good transparency.
- Liquid infused nanostructure of elastomer-based materials for outdoor applications have been considered.

### ARTICLE INFO

#### Keywords:

Anti-icing  
PDMS  
Slippery  
Lubricant  
Water repellency

### ABSTRACT

In this study, we conducted a facile method to fabricate an anti-icing surface on elastomer thin film by combining the PDMS nanostructure with the low surface tension lubricant. PDMS solution was mixed with slippery lubricant Krytox 1506 in a rational concentration and followed by a plasma dry etching process to promote the anti-icing performance in terms of shear stress and water repellency ability. Experimental results were compared with the reference substrates and demonstrated the advantages of the slippery surface in all mentioned scenarios. In addition, the functionalized surfaces also present high durability and good transparency, demonstrating a new facile method and design for outdoor anti-icing devices.

### 1. Introduction

Icing problems present an appreciable challenge in transportation safety, energy, and industrial. Ice accretion on the plane's wings and rear tail component might disrupt the airflow across the surface, mitigating the lift force [1–3]. Ice accumulation on energy transmission systems during winter leads to outages and massive collapse due to weight overloading, endangering people, and vehicles underneath [4–7]. Additionally, ice growth on ships and pavements can induce the slippage and subsequently cause accidents due to the unexpected loss of friction [8–10]. Anti-icing definitions have been intensively investigated to hinder effectively unexpected damages caused by ice accumulation and basically separated into two approaches. The active methods refer to the removal of existing ice using external energy such as heat, mechanical or melting solution. [11–15], while the passive approaches aim to prevent the ice formation without external energy by physicochemical methods [16–23]. Among the passive methods, superhydrophobic surfaces (SHs), which inspired by the lotus leaf and rose leaf structure, have been widely investigated in several decades and believed to be the

potential answer for anti-icing problems due to its precious behavior at the interface with liquid. Many reports have been introduced to optimize the anti-icing performance of SHs, including lowering the ice-surface affinity [9,24–26] or delaying the solidifying time [26–29]. However, recent studies have concluded that SHs cannot be the solution for anti-icing approaches due to its sensitivity with high humidity conditions and mechanical interlocking effect [30,31]. Water intrusion involves the anchoring of formed ice to the space between structure features, making it harder to remove than a smooth surface and consequently deteriorating the hydrophobic layer [32].

Inspired by the wall structure of *Nepenthes* pitcher plant [33], which is a combination of lunar-cells directed downward covered by a wax layer, Bioinspired Slippery Lubricant-Infused Porous surface (SLIP) has been recently introduced and believed to be an innovative icephobic solution [22,34–37]. This new anti-icing concept proposes a defect-free smooth liquid supported by a nanostructure underneath with superior properties in water repellency, high durability, self-healing, and humidity tolerance. Water droplets come in contact or condensed on the SLIP surface are elevated to the outer surface and isolated with surface

\* Corresponding author.

E-mail address: [ducnb@daihoctantrao.edu.vn](mailto:ducnb@daihoctantrao.edu.vn) (N.B. Duc).

<sup>1</sup> These authors contributed equally to this work.

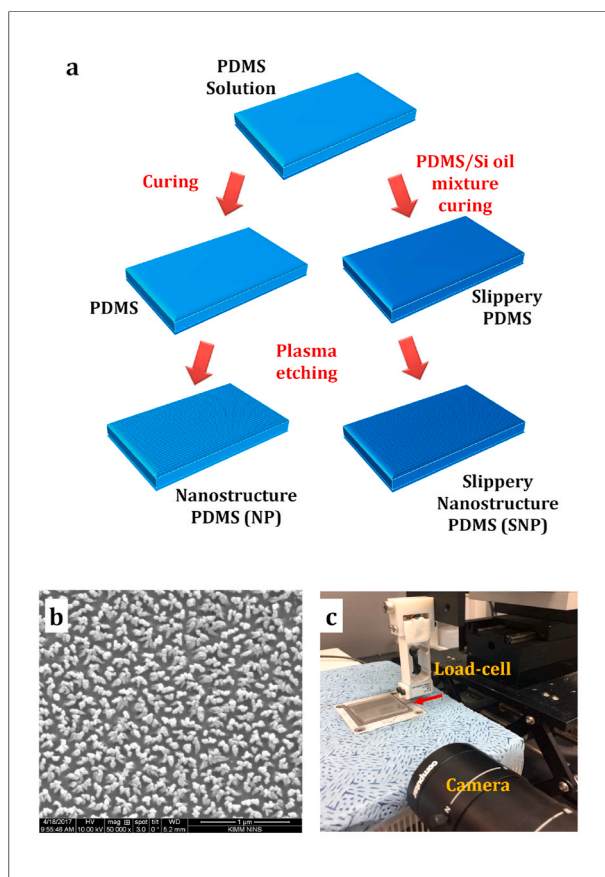


Fig. 1. The fabrication process of SP sample (a); nanopillars on PDMS surface after etching (b), shear stress measurement set-up (c).

features by a thin lubricant layer due to the immiscibility of water and lubricant, and subsequently facilitating the loose adhesion between surface structure and formed ice [23,38–40]. A SLIP surface can be achieved by combining a porous structure with a low-surface-tension lubricant, which is both immiscible in water and high affinity with rough surfaces. A typical porous surface can be made by various methods including dry/wet etching [23,41–44,45], lithography [43], or particle spraying [30], which aims to occupy the lubricant inside the structure. Various lubricants have been reported, such as FC-40, FC-70, silicone oil, or Krytox family with different viscosity and surface tension. SLIPs surface has been examined and demonstrated its advantages in anti-icing performance as the ease of removing formed ice or ice-free surface after exposure to icing conditions. However, there is no research until now dealing with elastomer surfaces for outdoor anti-icing purposes such as water repellency, durability, and optical performance.

In this work, we reinforced the anti-icing on slippery nanostructure PolyDimethylsiloxane (PDMS) thin film by accurately inject the industrial lubricant (Silicone oil) to elastomer solution with appropriate concentration. After the curing process, Slippery PDMS (SP) sample was bombarded by a plasma mixture of  $O_2$ ,  $H_2$ , and  $CF_4$  to generate the nanostructure on its surface. The anti-icing efficiency was evaluated in terms of shear stress, durability, and ice-endurance effectiveness. Results were compared with as-received quartz glass as a reference sample and demonstrated outstanding performance in all mentioned properties. Besides, the durability and optical performance of PDMS thin films were examined for outdoor applications. Our results propose a new convenient passive approach for anti-icing purposes and further investigations.

Table 1  
Information of examined surfaces.

Sample	Contact angle (degree)	Shear stress (kPa)	Ice appearance time (s) (covered on bare quartz)
Bare quartz	117	1355	80
PDMS	112	40	250
NP	102	86	282
SNP	104	10	–

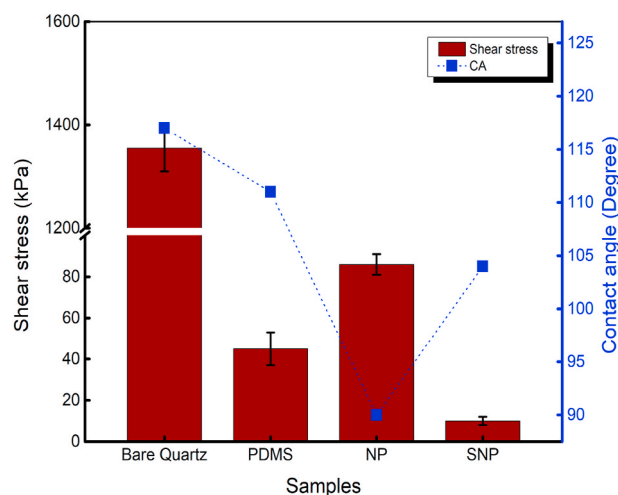


Fig. 2. Adhesive strength on different surfaces with bare Al as a reference sample and their corresponding wettabilities.

## 2. Materials and methods

The experiments were proceeded on PDMS (Merck KGaA, Darmstadt, Germany) rubber-based elastomer, as its popularity and basically possessed the good elasticity, and easily engrave. Fig. 1(a) describes the fabrication routine of examined samples in this study. The Slippery Nanostructure PDMS (SNP) sample was fabricated by mixing PDMS solution with curing material maintaining the weight ratio at 10:1. After well mixed, Si oil (Sigma Aldrich Co., Ltd.) was slowly added to the mixed solution to prepare a 3 wt% solution followed by a strict degassing step. After curing using a vacuum oven for 1 h, slippery thin-film was naturally dried in ambient air for another 1 h. Nanostructure was achieved by exposing the slippery thin film to the plasma mixture of  $O_2$ ,  $CF_4$ , and  $H_2$  in rational concentration. By controlling the etching time, we can generate the nanostructure with different shapes on the surface. On the other hand, Nanostructure PDMS (NP) sample also was fabricated by directly bombarded the PDMS thin film without any lubricant solution. The same nanostructure morphology was found on NP and SNP samples despite the presence of lubricant or not. The wettability of samples was observed using a contact angle measurement apparatus (Model DM-50, Kyowa Interface Science Co. Ltd.) with  $5\mu L$  deionized water droplets. The contact angle value (CA) was statistically averaged with at least five positions on each substrate. The information on examined surfaces can be found in Table 1.

Tested samples ( $100\mu m$ , 2.5 cm, and 2.5 cm in thickness, length, and width, respectively) were carefully attached to a thermoelectric cooling module by aluminum tape for shear stress measurement (Fig. 2). A  $5\mu L$  deionized water drop was gently dropped on the surface before started cooling down (setting temperature  $-10^\circ C$ ). A load-cell was used to determine the ice-surface shear stress. After freezing, load-cell controlled by a motorized stage moved at a constant speed ( $50\mu m/s$ ) and gently pushed the ice drop until it was detached. The force generated from the collision was obtained via computer software and

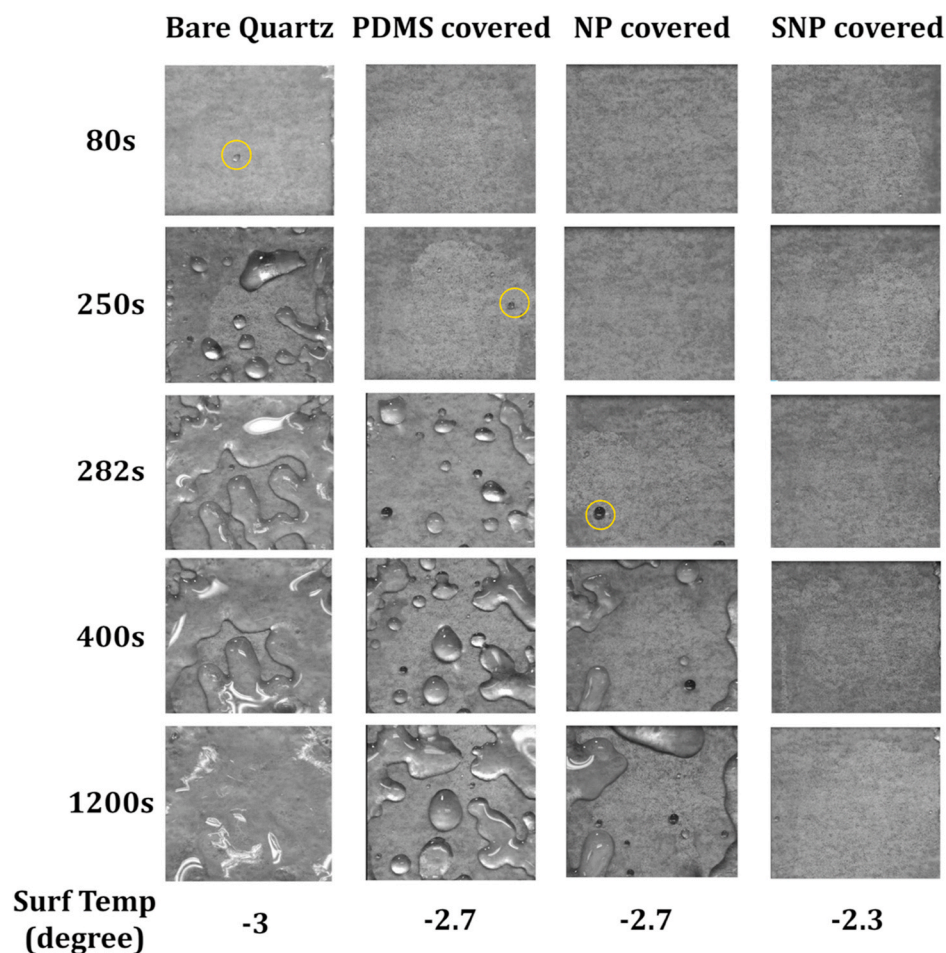


Fig. 3. The ice repellent efficiency on different surfaces.

statistically determined through the peak position in recorded data. A high-speed camera (Photron Co., Ltd.) was used to observe the icing process and measure the endurance time. A thermal couple was used to accurately measure the temperature at the interface when the phase transition occurred.

### 3. Results and discussion

The bonding mechanism between two adjacent substrates is attributed to the direct electrostatic interaction. In addition to chemical bonding and dispersion forces, two surfaces contain non-compensated or spatially separated charges will also generate electrostatic forces between electrical charges induced at the ice surface and solid substrate. Therefore, substrate-ice bulk adhesion can be degraded if we decrease the projected area or select rational materials. The second choice corresponds to the active method and seems to be infeasible owing to the popularity of materials such as glass, Cooper, or Aluminum. The most common passive approach has been named superhydrophobic. It was inspired by Lotus leaf's hierarchical structure integrated with a water-repellent wax to enhance the mobility of liquid on the surface. However, this old approach has been reported about the extremely low durability and bad performance in humid conditions. The SLIP concept is a new passive approach and aims to minimize the ice-surface adhesion owing to the remarkable behavior at the interface. This new definition illustrates a smooth defect-free interface supported by porous nanostructure underneath to elevate the water to the top and isolate it with surface features, this results in the transition from common feature-ice contact to lubricant-ice contact at the final state.

Fig. 3 describes the ice-surface shear stress on different materials

with bare quartz used as a reference sample. All PDMS-based thin films exhibit remarkable low shear stress compared to bare quartz (1355 kPa), which is attributed to the lower ice-substrate bonding strength. The shear stress measurement on PDMS-based surfaces is all below 100 kPa, opening a new selection for icephobic materials. The highest one belongs to the NP sample (86 kPa), which corresponds to 8.6 times higher than SNP and two times higher than the NP sample (Table 1). This can be explained by the water intrusion inside the nanostructure during the cooling process and results in the interlocking effect, which commonly found in nanostructured superhydrophobic surfaces. However, the shear stress on the PDMS NP sample is much lower than a nanostructure superhydrophobic textured on glass or Al substrate in our previous researches. This is due to the low electrostatic interaction between electrical charges and the elasticity of rubber-based material.

The measurement of shear stress on the original PDMS thin film emphasizes the disadvantages of nanostructure surface caused by the ice volume anchoring inside the surface structure. A flat surface ensures the not-low-but-stable shear stress due to the material originality (2 times lower than NP sample). However, the combination of nanostructure and lubricant warrants an outstanding anti-icing performance when it exhibits extremely low adhesion (10 kPa). This can be explained by the defect-free surface generated by a lubricant Si oil kept inside a nano-hair structure. Such a combination supports the high mobility state of ice drop on the surface for ease detaches. On the opposite side, the bare PDMS and NP without oil injection result in much higher value despite indicating the relatively same in contact angle. It should be noted here that the shear stress measurements carried on common materials such as glass, Cu, or Al are about 1000 kPa. Hence, this new concept might be considered for further applications not only by the originality of rubber-

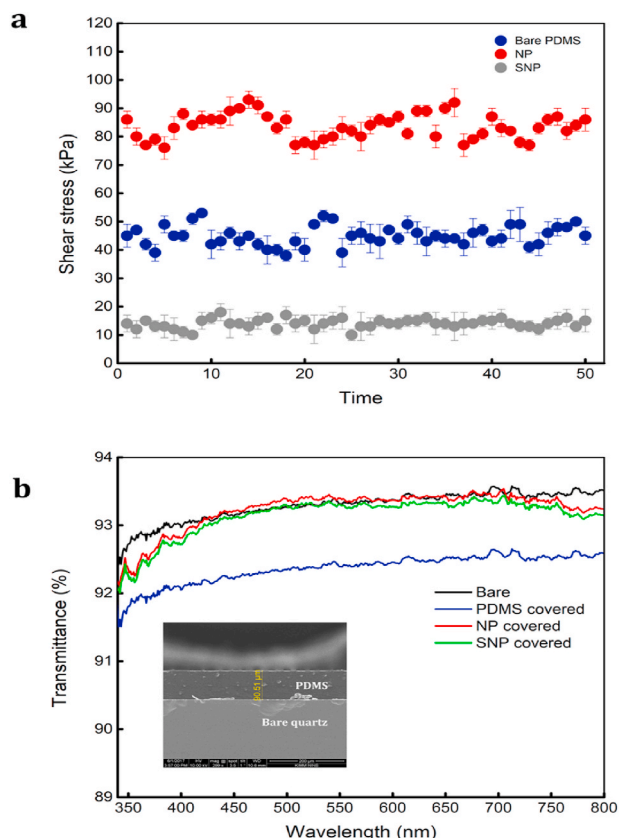


Fig. 4. Anti-icing durability (a) and optical performance (b).

based material but also by the rational incorporation between nanostructure and slippery lubricant.

For the outdoor and common appliances such as windshields or smart devices, ice-repelling and optical performance were statistically examined on bare glass - thin film covered samples. Samples were tilted at 90° and exposed to cold and humid airflow (temperature ~0 °C) while maintaining the sample temperature at -5 °C. A high-resolution camera was located opposite the sample's surface to observe the whole icing process. Fig. 3 presents the icing behavior in the real-time of the different thin films covered on bare glass. On the bare quartz sample, the apparent ice area was found early after exposure to the cooling flow (200s), which resulted from the condensation process. Water droplets

condensed on the surface rapidly coalesced with neighbor droplets to increase its volume and spread across the surface area before solidifying. This can be explained by a low heterogeneous nucleation energy barrier that strongly depends on surface energy. Bare quartz surface with high surface energy can easily support the generation of ice nuclei at a quite low surface temperature compared to the others. This situation also can be found in the NP sample when the ice area promptly occupied the surface area after a short time cooling (250 s). The low ice-repelling performance is attributed to the high surface area when water nuclei can be formed inside the nanostructure, unified, increased the volume, and subsequently solidified. On the opposite side, original PDMS with much lower exposed area illustrates better ice repelling efficiency than the NP sample when hindering the apparent ice volume up to 282 s after cooling. Nevertheless, the ice-covered area still can be seen easily on bare, PDMS covered and NP covered samples, which is attributed to the condensation and removal processes. Fortunately, those can be resolved by the SNP sample when it supports both the slippery and thermal delaying properties, and subsequently discloses the extreme ice repelling performance. As shown in Fig. 3, SNP thin film exhibits the outstanding ice repelling efficiency when hinders the ice nucleation and maintains the transparent surface after the 1200s of exposure (Table 1). This remarkable performance can be attributed to the slippery property and thermal conductivity of materials. The slippery property of the SNP surface supports the high mobility of condensed water droplets and facilitates the falling ability when reaches to the critical volume. Moreover, the low thermal conductivity of PDMS and lubricant inside the nanostructure cavities effectively delays the heat transfer across the sample, therefore increasing the energy barrier for nucleation at the surface. It should be noted here that the nucleation barrier energy is a sensitive function of surface temperature. The smaller the temperature difference (dew point - humid air for water condensation, and solidified - water temperature for ice nucleation), the higher the nucleation energy barrier. After 20 min of the experiment, SNP presented a clear surface without any ice formation and maintained for over 1-h experiments, demonstrating the great potential for outdoor applications.

Besides, the durability and optical performance of PDMS-based thin films also have been statistically examined. Fig. 4a describes the durability examination on three PDMS-based samples and reveals a negligible difference after 50 cycles with around 86 kPa, 44 kPa, 10 kPa on NP, PDMS, SP sample, respectively. Si oil discloses a good affinity with PDMS nanostructure and the self-healing property after a long time experiment. Additionally, transmittance spectra in the visible range also have been evaluated on glass - PDMS thin film covered and compared with bare glass (Fig. 4b). Because of the quite thin PDMS layer, the transparency of bare - PDMS covered samples slightly reduces to about

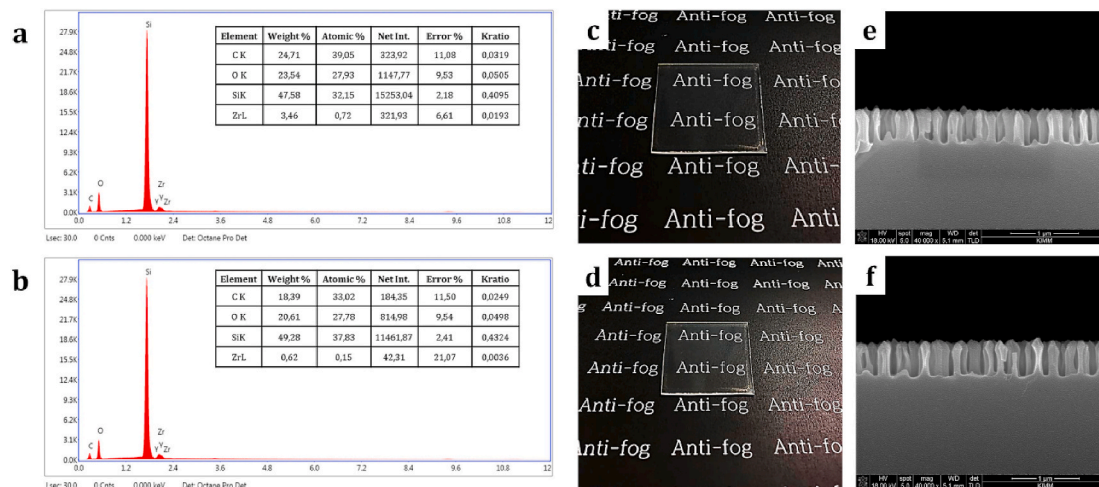


Fig. 5. EDX spectrum, transmittance and surface texture of SNP surface, respectively before (a,c,e) and after 50 cycles (b,d,f).

92.5%. Interestingly, the measurement of NP and SNP samples demonstrates the negligible difference with bare glass. This can be explained by the presence of an anti-reflection moth-eye structure, which enhances the transparency through the thin film. The inset Fig. 5 shows the SEM image of the PDMS thin layer on the glass surface. This remarkable property proposes the great potential for outdoor devices such as car windshield or commercial high rise windows. It also should be noted here that the quite good transparency of the lubricant layer presents a negligible effect on the optical properties.

#### 4. Conclusion

In this work, we investigated the anti-icing efficiency on slippery nanostructure PDMS thin film in several scenarios, including shear stress, durability, and ice-endurance performance. Nanostructure generated by the etching process exhibited a good affinity with low surface tension lubricant and showing the extremely low ice-surface adhesion, self-healing ability, and excellent icing repellency compared to the reference surface, emphasizing the advantages in icephobic solutions. Moreover, anti-icing durability and transmittance of glass – PDMS based thin film covered were examined and demonstrated the great potential for outdoor optical devices. This study aims to propose a new facile method and a paradigm for further investigations in anti-icing purposes.

#### Data availability statement

The data that support the findings of this study are available from the corresponding author upon reasonable request.

#### CRediT authorship contribution statement

**Nguyen Thanh Binh:** Formal analysis, Writing – review & editing.  
**Vu Thi Hong Hanh:** Writing – original draft, Writing – review & editing.  
**Ngo Tuan Ngoc:** Formal analysis, Writing – review & editing.  
**Nguyen Ba Duc:** Conceptualization, Writing – original draft, Formal analysis, Writing – review & editing.

#### Declaration of competing interest

The authors declare that they have no known competing financial interests or personal relationships that could have appeared to influence the work reported in this paper.

#### Acknowledgment

This research was funded by the Thai Nguyen University of Education under project number CS.2020.05. We also would like to express our thanks to Prof. Hyuneui Lim and Nature-Inspired Nanoconvergence System Department, Korea Institute of Machinery and Materials for valuable supports.

#### References

- [1] J. Marwitz, et al., Meteorological conditions associated with the ATR72 aircraft accident near Roselawn, Indiana, on 31 October 1994, *Bull. Am. Meteorol. Soc.* 78 (1997) 41–52.
- [2] P. Tran, M.T. Brahimi, I. Paraschivoiu, A. Pueyo, F. Tezok, Ice accretion on aircraft wings with thermodynamic effects, *J. Aircraft* 32 (1995) 444–446.
- [3] M. Sujata, M. Madan, K. Raghavendra, N. Jagannathan, S.K. Bhaumik, Unraveling the cause of an aircraft accident, *Eng. Fail. Anal.* 97 (2019) 740–758.
- [4] M. Farzaneh, Ice accretions on high-voltage conductors and insulators and related phenomena, *Philos. Trans. Math. Phys. Eng. Sci.* 358 (2000) 2971–3005.
- [5] J.L. Laforte, M.A. Allaire, J. Laflamme, State-of-the-art on power line de-icing, *Atmos. Res.* 46 (1998) 143–158.
- [6] D. Cerrai, M. Koukoulou, P. Watson, E.N. Anagnostou, Outage prediction models for snow and ice storms, *Sustain. Energy, Grids Networks* 21 (2020) 100294.
- [7] P.-O.A. Borrebæk, B.P. Jelle, Z. Zhang, Avoiding snow and ice accretion on building integrated photovoltaics – challenges, strategies, and opportunities, *Sol. Energy Mater. Sol. Cells* (2019) 110306, <https://doi.org/10.1016/j.solmat.2019.110306>.
- [8] A.-S. Milaković, F. Li, R.U.F. von Bock und Polach, S. Ehlers, Equivalent ice thickness in ship ice transit simulations: overview of existing definitions and proposition of an improved one, *Ship Technol. Res.* 1–17 (2019), <https://doi.org/10.1080/09377255.2019.1655260>.
- [9] Q. Wang, Z. Li, P. Lu, R. Lei, B. Cheng, 2014 Summer Arctic sea ice thickness and concentration from shipborne observations, *Int. J. Digit. Earth* 12 (2019) 931–947.
- [10] M. Landy, A. Freiburger, An approach to the shipboard icing problem, *Nav. Eng. J.* 80 (1968) 63–72.
- [11] J. Palacios, E. Smith, J. Rose, R. Royer, Ultrasonic de-icing of wind-tunnel impact icing, *J. Aircraft* 48 (2011) 1020–1027.
- [12] L. Makkonen, T. Laakso, M. Marjaniemi, K.J. Finstad, Modelling and prevention of ice accretion on wind turbines, *Wind Eng.* 25 (2001) 3–21.
- [13] X. Bu, G. Lin, X. Shen, Z. Hu, D. Wen, Numerical simulation of aircraft thermal anti-icing system based on a tight-coupling method, *Int. J. Heat Mass Tran.* 148 (2020) 119061.
- [14] E. Heymsfield, J.W. Daniels, R.F. Saunders, M.L. Kuss, Developing anti-icing airfield runways using surface embedded heat wires and renewable energy, *Sustain. Cities Soc.* 52 (2020) 101712.
- [15] P. Roberge, J. Lemay, J. Ruel, A. Bégin-Drolet, Field analysis, modeling and characterization of wind turbine hot air ice protection systems, *Cold Reg. Sci. Technol.* 163 (2019) 19–26.
- [16] L. Wang, et al., Robust anti-icing performance of silicon wafer with hollow micro-/nano-structured ZnO, *J. Ind. Eng. Chem.* 62 (2018) 46–51.
- [17] M. Wang, et al., A novel flexible micro-ratchet/ZnO nano-rods surface with rapid recovery icephobic performance, *J. Ind. Eng. Chem.* 62 (2018) 52–57.
- [18] G. Zhang, et al., Preparation of superhydrophobic films based on the diblock copolymer P(TFEMA-r-Sty)-b-PCEMA, *Phys. Chem. Chem. Phys.* 17 (2015) 19457–19464.
- [19] W. Hou, et al., Anti-icing performance of the superhydrophobic surface with micro-cubic array structures fabricated by plasma etching, *Colloids Surfaces A Physicochem. Eng. Asp.* 586 (2020) 124180.
- [20] W. Xing, et al., Anti-icing aluminum alloy surface with multi-level micro-nano textures constructed by picosecond laser, *Mater. Des.* 183 (2019) 108156.
- [21] X. Li, et al., Fabrication of bio-inspired non-fluorinated superhydrophobic surfaces with anti-icing property and its wettability transformation analysis, *Appl. Surf. Sci.* 505 (2020) 144386.
- [22] P. Kim, et al., Liquid-infused nanostructured surfaces with extreme anti-ice and anti-frost performance, *ACS Nano* 6 (2012) 6569–6577.
- [23] T.-B. Nguyen, S. Park, Y. Jung, H. Lim, Effects of hydrophobicity and lubricant characteristics on anti-icing performance of slippery lubricant-infused porous surfaces, *J. Ind. Eng. Chem.* 69 (2019).
- [24] L. Zhu, et al., Ice-phobic coatings based on silicon-oil-infused polydimethylsiloxane, *ACS Appl. Mater. Interfaces* 5 (2013) 4053–4062.
- [25] C.A. Martin, J.C. Putt, Advanced pneumatic impulse ice protection system (PIIP) for aircraft, *J. Aircraft* 29 (1992) 714–716.
- [26] T.-B. Nguyen, S. Park, H. Lim, Effects of morphology parameters on anti-icing performance in superhydrophobic surfaces, *Appl. Surf. Sci.* 435 (2018) 585–591.
- [27] B. Adanur, L. Cremaschi, E. Harges, Effect of mixed hydrophilic and hydrophobic surface coatings on droplets freezing and subsequent frost growth during air forced convection channel flows, *Sci. Technol. Built Environ.* 1–11 (2019), <https://doi.org/10.1080/23744731.2019.1648981>.
- [28] H. Guo, et al., Improving the anti-icing performance of superhydrophobic surfaces by nucleation inhibitor, *Surf. Eng.* 1–7 (2019), <https://doi.org/10.1080/02670844.2019.1677291>.
- [29] M. Grizen, T. Maitra, J.P. Bradley, M.K. Tiwari, Nanotextured aluminum-based surfaces with icephobic properties, *Heat Tran. Eng.* 1–10 (2019), <https://doi.org/10.1080/01457632.2019.1640461>.
- [30] F. Chu, X. Wu, L. Wang, Dynamic melting of freezing droplets on ultraslippery superhydrophobic surfaces, *ACS Appl. Mater. Interfaces* 9 (2017) 8420–8425.
- [31] S. Bengaluru Subramanyam, V. Kondrashov, J. Rühle, K.K. Varanasi, Low ice adhesion on nano-textured superhydrophobic surfaces under supersaturated conditions, *ACS Appl. Mater. Interfaces* 8 (2016) 12583–12587.
- [32] S. Jung, et al., Are superhydrophobic surfaces best for icephobicity? *Langmuir* 27 (2011) 3059–3066.
- [33] H.F. Bohn, W. Federle, Insect aquaplaning: *Nepenthes* pitcher plants capture prey with the peristome, a fully wettable water-lubricated anisotropic surface, *Proc. Natl. Acad. Sci. U.S.A.* 101 (2004) 14138–14143.
- [34] N. Wang, et al., Design and fabrication of the lyophobic slippery surface and its application in anti-icing, *J. Phys. Chem. C* 120 (2016) 11054–11059.
- [35] F. Arianpour, M. Farzaneh, S.A. Kulinich, Hydrophobic and ice-retarding properties of doped silicone rubber coatings, *Appl. Surf. Sci.* 265 (2013) 546–552.
- [36] L. Yin, et al., In situ investigation of ice formation on surfaces with representative wettability, *Appl. Surf. Sci.* 256 (2010) 6764–6769.
- [37] P.W. Wilson, et al., Inhibition of ice nucleation by slippery liquid-infused porous surfaces (SLIPS), *Phys. Chem. Chem. Phys.* 15 (2013) 581–585.
- [38] K.K. Varanasi, T. Deng, J.D. Smith, M. Hsu, N. Bhate, Frost formation and ice adhesion on superhydrophobic surfaces, *Appl. Phys. Lett.* 97 (2010) 234102.
- [39] C. Stamatopoulos, J. Hemrle, D. Wang, D. Poulidakos, Exceptional anti-icing performance of self-impregnating slippery surfaces, *ACS Appl. Mater. Interfaces* 9 (2017) 10233–10242.
- [40] N. Wang, et al., Robust superhydrophobic coating and the anti-icing properties of its lubricants-infused-composite surface under condensing condition, *New J. Chem.* 41 (2017) 1846–1853.

- [41] T. Wang, et al., Passive anti-icing and active deicing films, *ACS Appl. Mater. Interfaces* 8 (2016) 14169–14173.
- [42] L. Wang, Q. Zhou, Y. Zheng, S. Xu, Composite structure and properties of the pitcher surface of the carnivorous plant *Nepenthes* and its influence on the insect attachment system, *Prog. Nat. Sci.* 19 (2009) 1657–1664.
- [43] T.-S. Wong, et al., Bioinspired self-repairing slippery surfaces with pressure-stable omniphobicity, *Nature* 477 (2011) 443–447.
- [44] P. Juuti, et al., Achieving a slippery, liquid-infused porous surface with anti-icing properties by direct deposition of flame synthesized aerosol nanoparticles on a thermally fragile substrate, *Appl. Phys. Lett.* 110 (2017) 161603.
- [45] S.B. Subramanyam, K. Rykaczewski, K.K. Varanasi, Ice adhesion on lubricant-impregnated textured surfaces, *Langmuir* 29 (2013) 13414–13418.